Available online at www.sciencedirect.com
ScienceDirect
Earth and Planetary Science Letters 268 (2008) 202–211
EPSL
www.elsevier.com/locate/epsl

Modeling the effect of abrupt ocean circulation change on marine reservoir age

Stefan P. Ritz [a,b,*], Thomas F. Stocker [a,b], Simon A. Müller [a,1]

[a] Climate and Environmental Physics, Physics Institute, University of Bern, Bern, Switzerland
[b] Oeschger Centre for Climate Change Research, University of Bern, Bern, Switzerland

Received 5 July 2007; received in revised form 15 January 2008; accepted 15 January 2008
Available online 4 February 2008
Editor: M.L. Delaney

Abstract

Radiocarbon surface reservoir age is required for precise dating of marine organisms. Although often assumed constant, changes in atmospheric radiocarbon content, ocean circulation, and ocean mixing imprint changes on this quantity. The spatial and temporal variations of marine surface and bottom reservoir ages in response to a shutdown and subsequent recovery of Atlantic meridional overturning circulation (MOC) are analyzed using a cost-efficient, three-dimensional ocean circulation model. Generally, surface reservoir age changes are limited to the Atlantic Ocean with a reduction of about 100 yr after the MOC shutdown, followed by a slow increase and a peak at the time of MOC resumption. Parameter sensitivity studies with respect to the roles of gas exchange, diffusivity and North Atlantic ice cover show that ice cover has the largest effect on the transient evolution of surface reservoir age during the shutdown. Our model results agree well with a recent reconstruction of surface reservoir age changes during the Younger Dryas when we reduce the rate of gas exchange in the model and include a parametrization of seasonal ice cover in the North Atlantic.

Keywords: reservoir age; Younger Dryas; radiocarbon; MOC; overturning; circulation

1. Introduction

Knowing the marine surface reservoir age, defined as the difference in the ^{14}C age between the atmosphere and the surface ocean, is essential for dating purposes in marine archives such as sediment cores and corals. Hereafter, it will be referred to as reservoir age. For instance, terrestrial organic matter is dated using ^{14}C. Due to changes in the carbon cycle and in the production rate of ^{14}C over time, a ^{14}C calibration curve is used to convert ^{14}C age to calendar age (Reimer et al., 2004; Fairbanks et al., 2005). In order to date surface ocean biogenic matter, such as planktonic foraminifera found in sediment cores, an equivalent calibration curve for the surface ocean is needed. Since this is not available, the calibration curve for the atmosphere is used and an estimated reservoir age is added (Stuiver and Braziunas, 1993), often assumed to be constant and similar to modern, bomb-corrected reservoir ages.

The purpose of this paper is to provide information on spatial and temporal differences of reservoir age during abrupt climate change by using a cost-efficient, zonally resolved ocean model (Müller et al., 2006). We investigate the fingerprint of a shutdown of the Atlantic meridional overturning circulation (MOC) on surface and bottom reservoir ages and examine the reservoir age sensitivity to various model parameters.

In a recent study, Bondevik et al. (2006) presented a continuous record of reservoir age changes before, during and after the Younger Dryas (YD) stadial (approximately 12.8 to 11.6 ka before present (BP, before 1950); Gulliksen et al., 1998;

* Corresponding author. Climate and Environmental Physics, Physics Institute, University of Bern, Bern, Switzerland.
E-mail address: ritz@climate.unibe.ch (S.P. Ritz).
[1] Now at Earth and Environmental Sciences, Open University, Milton Keynes, UK.

0012-821X/$ - see front matter © 2008 Elsevier B.V. All rights reserved.
doi:10.1016/j.epsl.2008.01.024

Hughen et al., 2000; Friedrich et al., 2004; Southon, 2004), comparing ^{14}C ages of terrestrial plant fragments and marine shells found in the same sediment cores on Norway's west coast. They found an increase in reservoir age from 400 to 600 yr in the early YD and a drop by 300 yr immediately following the YD–Holocene transition. Earlier modeling studies have analyzed the response of reservoir age to sea ice cover, wind speed and Atlantic MOC changes using simple box models and zonally averaged Earth system models (Bard et al., 1994; Stocker and Wright, 1996, 1998; Delaygue et al., 2003). They found changes of more than 400 yr in the North Atlantic attributed to changes in convection and sea ice coverage. When the North Atlantic is ice covered for ten months out of the year, gas exchange flux is significantly reduced, thus contributing to an increase in reservoir age of 200 to 300 yr (Bard et al., 1994). In a modeling study using a three-dimensional ocean model, Butzin et al. (2005) found bottom reservoir age variations of up to 1000 yr in the North Atlantic when the MOC shuts down. For the surface reservoir age, they did not find the increase reported by Bard et al. (1994). Here, we address changes in the surface and bottom reservoir age distribution to YD type events and compare the results to the reservoir age reconstructions of Bondevik et al. (2006).

2. Model setup and simulations

For this study we use the Bern3D ocean model, a cost-efficient, seasonally forced, three-dimensional frictional geostrophic ocean model (Müller et al., 2006). It consists of 36×36 grid boxes in the horizontal direction and 32 layers in depth. The model is run under mixed boundary conditions for temperature and salinity. The temperature fields are taken from Levitus and Boyer (1994), and the salinity fields from Levitus et al. (1994). The atmosphere is described by one well-mixed box. Air–sea gas transfer velocity and a climatology of fractional sea ice cover for the modern climate, based on the OCMIP-2 protocol (Walsh, 1978; Zwally et al., 1983; Orr, 1999), modulate the atmosphere-to-ocean ^{14}C flux. In the ocean model, ^{14}C is transported as $^{14}R = {}^{14}C/{}^{12}C$. The ^{12}C concentration for the atmosphere (pCO_2) and the ocean (total inorganic carbon) are held constant at the pre-industrial values of 278 ppm and 2 mol m^{-3}, respectively. The ^{14}C production rate in the atmosphere is held constant as well. Thus, we do not account for changes in solar activity and geomagnetic field intensity. A 26,000-yr spinup, which includes diagnostics of the salinity fields for the mixed boundary conditions and ^{14}C production rate, preceded all simulations of this study. The spinup is required in order to obtain a steady state solution for the ^{14}C distribution. In order to diagnose the ^{14}C production rate, atmospheric $\Delta^{14}C$ is held constant. At steady state, the production rate in the model is then equal to the decay of the ^{14}C content in the atmosphere and the ocean.

First, a steady state control run (CTRL) has been performed. It will be addressed throughout the paper when comparisons to the steady state are made. Next we present a simulation, STDR, in which freshwater was injected into the Greenland–Iceland–Norwegian (GIN) sea (Tarasov and Peltier, 2005) from 30 to 0°W and 55 to 70°N for 200 yr with a triangular evolution in time (Fig. 2c). The freshwater pulse shuts down the Atlantic MOC resulting in a reversed overturning circulation in the model (Fig. 1g). Further simulations with larger pulses have shown that besides the effect of the MOC shutdown, the perturbation has an effect on the Antarctic Bottom Water cell and hence on the ^{14}C distribution, which leads to larger long-term changes in reservoir age. Here we are primarily interested in the effect of the MOC shutdown. In contrast to most complex ocean models, our model has multiple equilibrium states for the current parameter settings. This requires a negative freshwater perturbation in order for the MOC to recover (Fig. 2c). The MOC recovery was triggered to occur 1200 yr after the shutdown; this is comparable to the duration of the YD. Similar to the freshwater pulse which causes the MOC shutdown, this perturbation may have direct model-specific responses on ^{14}C. But in contrast to many simpler ocean models, the MOC does not overshoot when recovered from the shutdown state by a negative freshwater perturbation (e.g., Stocker and Wright, 1996).

For parameter sensitivity studies, five additional simulations have been performed with an MOC scenario similar to STDR. First, in a run referred to as KGAS, the air–sea gas transfer velocity used in OCMIP-2 (Orr, 1999) was reduced by 19%, as suggested by Müller et al. (in press). In a second run, which will be referred to as PCO2, atmospheric pCO_2 was reduced to 238 ppm. This corresponds to the value at the onset of the YD (Monnin et al., 2001). In a manner similar to the gas transfer velocity, pCO_2 affects the ^{14}C exchange flux between the atmosphere and the ocean. In the third run the diapycnal diffusivity was increased from 10^{-5} m^2 s^{-1} to $4 \cdot 10^{-5}$ m^2 s^{-1} (DIFF). This increases the maximum annual-mean MOC value from 14.0 Sv (Sverdrup; 1 Sv = 10^6 m^3 s^{-1}) in STDR to 16.5 Sv, and thus allows us to investigate whether an MOC shutdown from this higher state results in a larger reservoir age change. Since a higher diapycnal diffusivity strengthens top-to-bottom mixing, we expect to see higher surface reservoir ages. Because diapycnal diffusivity is an important model tuning parameter, it is important to understand its effects on reservoir age. Note that the parameters discussed so far are held constant throughout the run and do not vary when the MOC changes. In order to start the simulations from steady state, a separate spinup preceded each of these runs.

In two runs the effect of sea ice on reservoir age is considered. Since the presence of sea ice hinders equilibration of atmospheric and surface ocean ^{14}C concentrations, higher reservoir ages are expected in regions covered by sea ice. In these runs we additionally prescribed a fractional sea ice cover in the Northern Hemisphere which we will refer to as "equivalent sea ice cover". Because the model does not include a dynamic sea ice component, we simulated its effect on ^{14}C by artificially setting the atmosphere–ocean ^{14}C transfer to zero in the Arctic Ocean and in the Atlantic north of 63°N in run ICE1 (which matches estimates of the sea ice extent for the YD by Koç et al., 1993), and north of 56°N in run ICE2, respectively. This equivalent sea ice cover does not affect the exchange of heat and freshwater. Equivalent sea ice is activated, i.e. ^{14}C

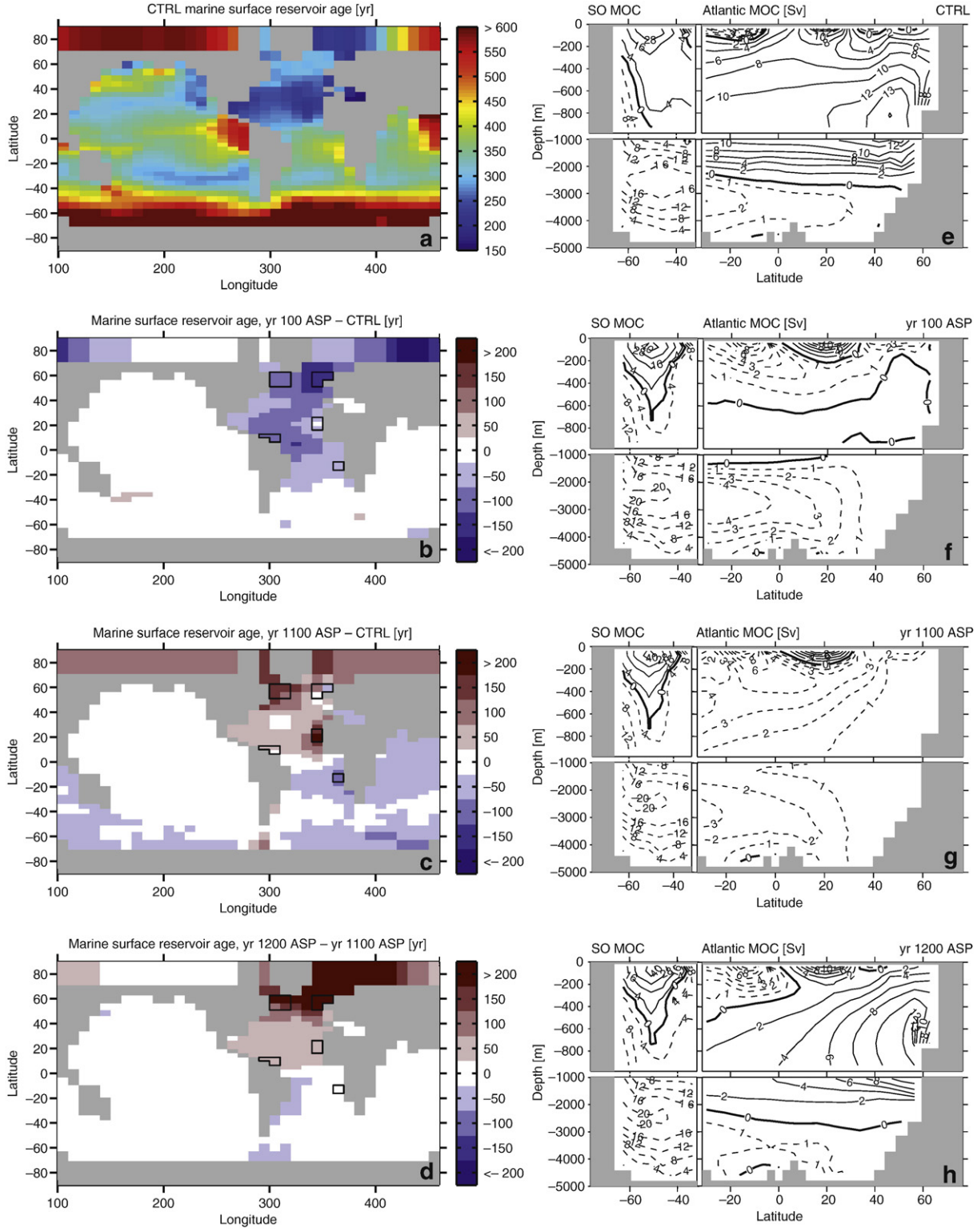

Fig. 1. a, Marine surface reservoir age distribution of CTRL. Large reservoir ages occur in regions of upwelling of old, ^{14}C-depleted deep waters, whereas regions of deep water formation and subduction show young ages. b–d, STDR marine surface reservoir age anomalies. Marked in black outlines are the regions of largest changes as well as the region of the Cariaco basin and Barbados; b, Short-term variations due to the Atlantic meridional overturning circulation (MOC) shutdown (100 yr after the start of the perturbation (hereafter referred to as ASP) compared to CTRL); c, Long-term variations due to the MOC shutdown (year 1100 ASP compared to CTRL); d, Short-term variations due to the recovery of the MOC (change in reservoir age between year 1100 ASP and year 1200 ASP). e–h, Southern Ocean (SO) and Atlantic MOC (in Sv, 1 Sv = 10^6 m^3 s^{-1}) for CTRL, year 100 ASP, year 1100 ASP and year 1200 ASP; g, the MOC is reversed during the "off" state.

exchange is suppressed, when the maximum Atlantic MOC sinks below 7 Sv. The suppression is removed when MOC strength rises above this threshold. The equivalent sea ice cover remains seasonally constant. Note that this equivalent sea ice is in addition to the modern OCMIP-2 sea ice coverage and does not replace it. The timing of the freshwater perturbations for all runs mentioned above is the same as in STDR and summarized in Table 1.

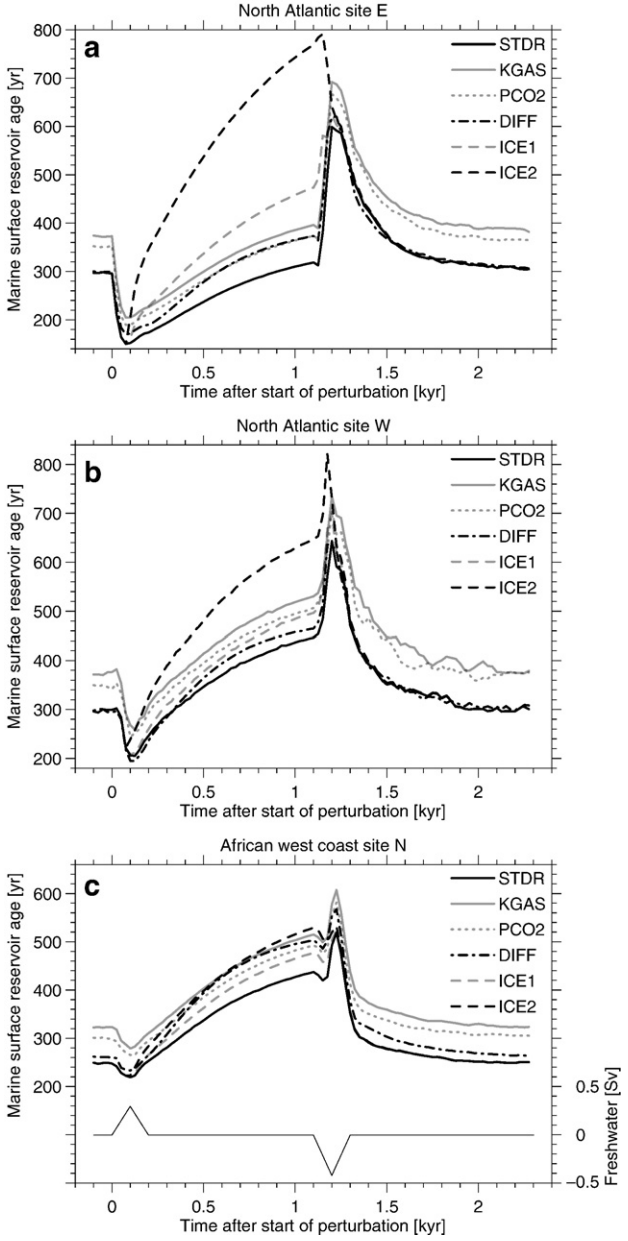

Fig. 2. Marine surface reservoir age time series of STDR and its behavior to a reduced air–sea gas transfer velocity by 19% (KGAS), reduced atmospheric pCO_2 to the pre-YD value of 238 ppm (PCO2), increased diapycnal diffusivity from 10^{-5} m^2 s^{-1} to $4\cdot10^{-5}$ m^2 s^{-1} (DIFF), and to increased sea ice cover when in circulation "off" state (ICE1 and ICE2, seasonally constant equivalent ice cover north of 63°N and north of 56°N, respectively) (Table 1) for the North Atlantic site E (a), the North Atlantic site W (b) and the African west coast site N (c). The timing and amount of the freshwater perturbations are indicated in panel c. Note that DIFF needs a larger maximum negative freshwater perturbation of −0.56 Sv for the MOC to recover (see Table 1).

Table 1
Summary of the model simulations

Simulations	Notes	F_{pos}^{max}	F_{neg}^{max}
CTRL	5000 yr steady state (control) run	–	–
STDR	Standard run	0.3 Sv	−0.42 Sv
KGAS	Air–sea gas transfer velocity reduced by 19%	0.3 Sv	−0.42 Sv
PCO2	Atmospheric pCO_2 reduced from 278 ppm to 238 ppm	0.3 Sv	−0.42 Sv
DIFF	Diapycnal diffusivity increased from 10^{-5} m^2 s^{-1} to $4\cdot10^{-5}$ m^2 s^{-1}	0.3 Sv	−0.56 Sv
ICE1	Equivalent sea ice cover (north of 63°N) added during the shutdown state	0.3 Sv	−0.42 Sv
ICE2	Equivalent sea ice cover (north of 56°N) added during the shutdown state	0.3 Sv	−0.42 Sv
BEST	Air–sea gas exchange as in KGAS, pCO_2 as in PCO2, equivalent sea ice cover as in ICE1	0.3 Sv	−0.42 Sv

Except for CTRL, all simulations have a duration of 2400 yr with a triangular freshwater perturbation starting 100 yr after the start of the run and lasting for 200 yr (Fig. 2c). The negative freshwater perturbation starts at year 1100 after the beginning of the positive freshwater perturbation and lasts for 200 yr. F_{pos}^{max} and F_{pos}^{max} stand for the maximum positive and negative freshwater input fluxes of the perturbations.

Marine surface reservoir age (τ_s) is defined as

$$\tau_s = \frac{1}{\lambda}\ln\left(\frac{^{14}R_{atm}}{^{14}R_{oc}(z=0)}\right), \quad (1)$$

marine bottom reservoir age as

$$\tau_b = \frac{1}{\lambda}\ln\left(\frac{^{14}R_{atm}}{^{14}R_{oc}(z=-H)}\right), \quad (2)$$

where $\lambda = 1/8267$ yr^{-1} is the decay constant for ^{14}C (Godwin, 1962), and $^{14}R_{atm}$ and $^{14}R_{oc}(z)$ are the ^{14}C to ^{12}C ratios for the atmosphere, surface ocean ($z=0$) and bottom ocean ($z=-H$), respectively. H represents the depth of the water column and varies spatially. As the surface ocean ^{14}C concentration is determined by measuring ^{14}C of planktonic foraminifera, $^{14}R_{oc}$ is actually the mean ^{14}C concentration of the euphotic zone, whose depth varies spatially from a few meters to around 200 m in the open ocean. In the model, $^{14}R_{oc}(z=0)$ is derived by taking the mean concentration of the top two layers which correspond to a depth of approximately 80 m. ^{14}C concentrations are expressed in ‰ as

$$\Delta^{14}C = \left(\frac{^{14}R}{^{14}R_{st}} - 1\right)\cdot 1000‰, \quad (3)$$

where $^{14}R_{st} = 1.176\cdot10^{-12}$ is the pre-industrial atmospheric ^{14}C to ^{12}C ratio (Karlén et al., 1964). In CTRL we set the atmospheric Δ^{14}C to 0‰.

3. Reservoir age response to freshwater forcing

3.1. Steady state and general temporal evolution of reservoir age

Simulation CTRL displays a wide range of surface reservoir ages from about 250 yr in the Atlantic from 10 to 50°N to over

600 yr in the Indian and Southern Oceans and in the eastern equatorial Pacific (Fig. 1a). As the atmospheric ^{14}C concentration is spatially constant, the variations reflect spatial differences in ocean concentrations. High reservoir ages correlate with upwelling regions where old, ^{14}C-depleted waters reach the surface. In the Arctic Ocean, the high reservoir ages are due to a combination of sea ice cover and a low horizontal mixing rate.

In order to detect regions with high reservoir age changes during the YD, reservoir ages of CTRL and of STDR were compared to one another shortly after the MOC shutdown (100 yr after the start of the perturbation, hereafter referred to as ASP), as well as 1100 yr ASP, shortly before MOC resumption (short-term variations, Fig. 1b and long-term variations, Fig. 1c, respectively). In a second step the short-term variations due to the MOC recovery in STDR were analyzed (year 1200 ASP compared to year 1100 ASP, Fig. 1d). For the short-term variations due to the shutdown, reservoir ages decrease in the entire Atlantic by about 100 yr (Fig. 1b). The Southern, Indian and Pacific Oceans remain mostly unaffected. The Northern Hemisphere Atlantic reservoir age increases to values greater than those in CTRL for the long-term variation (Fig. 1c). The largest changes are found north of 50°N in the western Atlantic and at the North African west coast from 10 to 30°N. In the Southern Hemisphere the African west coast from 5 to 20°S shows the highest changes of around 100 yr compared to CTRL. The Southern and Indian Ocean reservoir ages decrease during this step by approximately 50 yr. The short-term reservoir age changes due to the recovery of the Atlantic MOC mainly consist of a large increase in the North Atlantic of up to 400 yr (Fig. 1d).

3.2. Regions with particularly large reservoir age variations

The evolution of the reservoir ages is investigated further in regions with particularly large age variations. These are the northwest and northeast Atlantic, as well as the northern and southern west coast of Africa (regions marked in Fig. 1).

The three Northern Hemisphere Atlantic sites show similar behavior (Fig. 2): A drop in reservoir age directly after the shutdown of the MOC is followed by an increase to higher values than in CTRL. The ocean has not reached steady state yet at the time of the negative freshwater perturbation. This perturbation results in a very fast and large reservoir age increase followed by a decrease to CTRL reservoir ages. The reservoir age of the southern site of the African west coast (Fig. 3) drops rapidly by 150 yr and increases afterwards slowly by 30 to 40 yr. The negative freshwater perturbation then brings the reservoir ages back to the values of CTRL.

In the following, the reasons for the modeled reservoir age changes are discussed in more detail for these regions on the basis of STDR.

For North Atlantic site W, after the Atlantic MOC shutdown, surface waters remain at the surface of the ocean and have more time to take up ^{14}C from the atmosphere. This increases the concentration in the surface ocean and consequently atmospheric $\Delta^{14}C$. The rise of both atmospheric and surface ocean ^{14}C concentrations, and the fact that the ocean increase leads the atmospheric increase (Fig. 4), results in a brief decrease of the reservoir age in the entire Atlantic, especially along the path of the southward flowing waters. This can be derived from Eq. (1).

In the model, the Atlantic MOC is reversed when in the "off" state (Fig. 1g), creating a region of upwelling in the northwestern Atlantic. As a result, reservoir age in this region increases. The longer the MOC remains in the "off " state, waters that are more depleted in ^{14}C reach the surface. Hence, reservoir age increases until the negative freshwater perturbation is added and the MOC recovers. At this time, convection recommences, resulting in the transport of a large amount of deep water to the surface very quickly. This results in an abrupt reservoir age increase of about 300 yr.

After the MOC shutdown, reservoir age decreases at North Atlantic site E for the same reasons as at site W. Here too, the reservoir age increases during the second stage. In contrast to

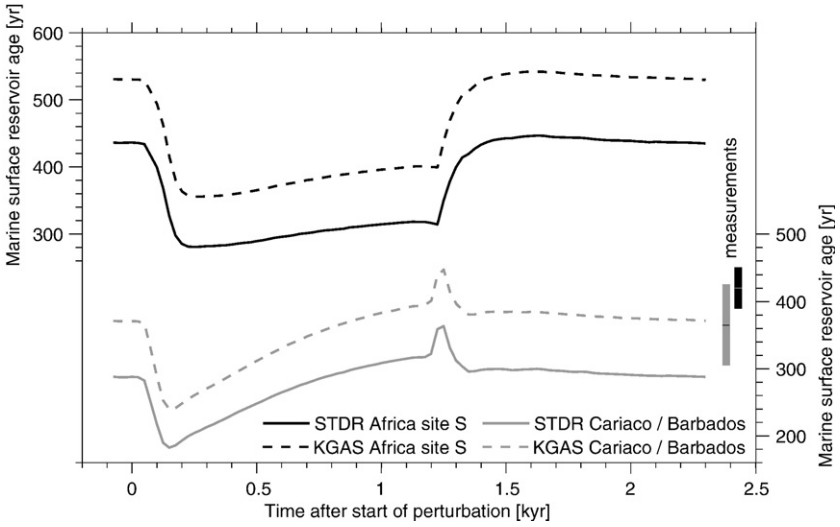

Fig. 3. Evolution of the marine surface reservoir age for the African west coast site S and the Cariaco basin/Barbados in STDR and KGAS. The reduced air–sea gas transfer velocity in KGAS leads to a better match between the control reservoir ages and modern reservoir age measurements for the Cariaco basin (indicated by the black vertical bar; Hughen et al., 2004), and averaged Holocene measurements for Barbados (gray vertical bar; Fairbanks et al., 2005), respectively.

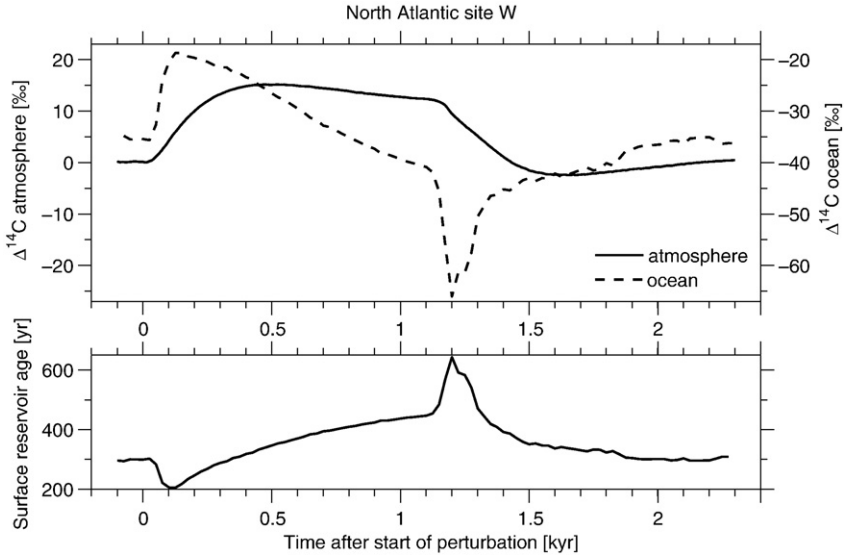

Fig. 4. Atmospheric and surface ocean $\Delta^{14}C$ (upper panel) and marine surface reservoir age (lower panel) for North Atlantic site W of STDR. Large changes in reservoir age occur when atmospheric and surface ocean $\Delta^{14}C$ behave differently. For instance, the reservoir age drop at the onset of the YD can be assigned to the fact that the ocean $\Delta^{14}C$ increase leads the atmospheric increase.

the northwestern Atlantic, this is due to the advective surface flux and mixing processes, which transport old waters from west to east. The reservoir age increase is not as steep as at site W, probably explained by the mixing processes of the eastward flowing waters.

At site N off the African west coast, upwelling becomes dominant during the "off " state. After a small drop in reservoir age, old waters start reaching the surface and continuously increase reservoir age. The slow reservoir age increase continues until the MOC recovers. The subsequent abrupt reservoir age change is influenced by two effects: The southward flow of low $\Delta^{14}C$ surface waters, which increases reservoir age and the weakening of the upwelling in this region, which leads to a reservoir age decrease.

During the MOC "on" state (i.e., in CTRL) strong upwelling in the Atlantic prevails only at the African west coast site S. Therefore, the CTRL reservoir age is remarkably higher than elsewhere in the Atlantic Ocean (Figs. 1a and 3). Upwelling is interrupted during the "off " state. The reservoir age adapts to the adjacent values, which are much lower. After the abrupt reservoir age drop, it increases slightly as the ocean approaches a new steady state. The upwelling recovers when the MOC switches on again, and the reservoir age rises to its CTRL value.

3.3. Reservoir age response in the Caribbean

^{14}C calibrations such as those of Reimer et al. (2004) and Fairbanks et al. (2005) are based on ^{14}C-measurements in tree rings extending back to approximately 12 ka BP. For the YD period and beyond, the Reimer et al. (2004) calibration is based on ^{14}C data from marine varves from the Venezuelan Cariaco basin (Hughen et al., 2000) (two sediment cores at 10.7°N 65.0°W) and on corals from various locations. The reconstruction of Fairbanks et al. (2005) is based on corals from an offshore reef core collection from Barbados (at 13.1°N 157.8°W). In order to link these marine data to the atmospheric values, a constant reservoir age of 420 yr is used for the Cariaco basin, while a constant reservoir age of 365 yr is used for the Barbados corals. Other work by Kromer et al. (2004), based on a floating tree-ring chronology, report higher reservoir ages for the Cariaco basin during the Allerød and a reservoir age drop of approximately 200 yr at the onset of the YD. A larger drop is reported by Muscheler et al. (in press).

In our model the reservoir age for the Cariaco and the Barbados regions (Fig. 3, region marked in Fig. 1) drops by approximately 100 yr at the onset of the YD followed by a slower increase to values larger than in CTRL. The abrupt recovery shows only a short rise of about 50 yr before decreasing again to its CTRL value.

3.4. Marine bottom reservoir age

Bottom reservoir age is of importance for dating benthic foraminifera from sediment cores. Analogous to the surface reservoir age, the short- and long-term bottom reservoir age variations due to the MOC shutdown and the short-term variations to the MOC recovery are discussed here (Fig. 5). The short-term bottom reservoir age changes to the MOC shutdown are less than 100 yr in most parts of the global ocean (Fig. 5a). A bottom reservoir age increase of more than 200 yr occurs only south of Greenland, where convection ceases abruptly and the ventilation in the water column is cut off. The largest increase of 780 yr is also found in this region.

The long-term anomalies (comparison of 1100 yr ASP to CTRL, Fig. 5b) show a distribution similar to the short-term anomalies, but changes are larger. Again, in the entire Pacific, Indian and Southern Oceans the marine bottom reservoir age remains constant. A small reservoir age decrease of 100 to 200 yr is found in the low latitude Atlantic Ocean. The largest increases of 1000 to 1500 yr occur in the Caribbean Sea and the

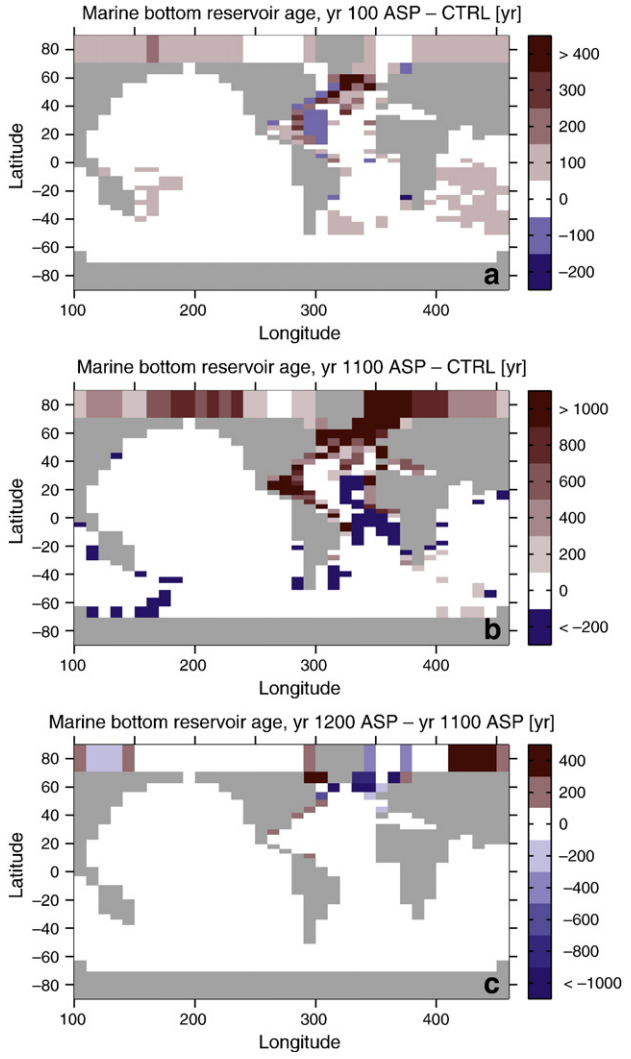

Fig. 5. STDR marine bottom reservoir age anomalies. a, Short-term variations due to the Atlantic MOC shutdown (year 100 after the start of the perturbation (ASP) compared to CTRL). b, Long-term variations due to the MOC shutdown (year 1100 ASP compared to CTRL). c, Short-term variations due to the recovery of the MOC (change in reservoir age between year 1100 ASP and year 1200 ASP). Note that the color bars of the panels are not identical.

Gulf of Mexico as well as South of Greenland, where the model shows bottom reservoir ages up to 1700 yr older than in CTRL. This reservoir age increase throughout the YD can be explained by the ^{14}C decay of these waters, which are not advected away in this state of the overturning circulation (Fig. 1g).

The MOC recovery causes an abrupt bottom reservoir age decrease of 700 to 1000 yr to the southeast of Greenland where convection reappears, which restarts the ventilation process in the water column (Fig. 5c). The bottom reservoir age increase southwest of Greenland is primarily a signal from the surface ocean, since the average depth of this region is only 320 m (see also Fig. 1d). Because the model simulations start and end in the modern state, the long-term reservoir age anomalies due to the MOC recovery are the reverse of those produced when the MOC shuts down.

In a previous modeling study using the UVic Earth System Climate Model, Meissner et al. (2003) analyzed top-to-bottom ^{14}C ages as a function of the Atlantic MOC strength. In agreement with our results, they found largest changes in the Caribbean Sea of approximately 1000 yr after a shutdown of the MOC. Similar results were reported by Butzin et al. (2005).

4. Parameter sensitivities

In addition to STDR, we have run the model with various alternative parameter settings as described in the model section (Fig. 2). In KGAS, the simulation with the reduced air–sea gas transfer velocity, we find an 80 to 100 yr shift to higher reservoir ages in all three regions. This change is expected, because a slower air–sea gas exchange increases the ^{14}C concentration difference between the atmosphere and the ocean, which by definition corresponds to a higher reservoir age. When running the model with the pre-YD atmospheric pCO_2 value of 238 ppm instead of 278 ppm (PCO2), reservoir age results in values 50 to 80 yr higher than in STDR in all three regions. Since the air–sea gas transfer velocity and pCO_2 both affect the air–sea gas exchange, their effect on reservoir age is very similar. According to Monnin et al. (2001) pCO_2 increases approximately linearly to 265 ppm during the YD. Accounting for this pCO_2 change over time would result in a linear reduction of the reservoir age offset between PCO2 and STDR (not shown here).

For DIFF, control state reservoir ages are approximately 50 yr higher in the Indian Ocean and 50 to 100 yr higher in the Pacific compared to STDR. The largest anomalies of approximately 150 yr are found north of Australia. Reservoir ages are 100 to 200 yr lower off the coast of Antarctica. For the long-term variations due to the shutdown of the MOC, the reservoir age increase is about 50 yr larger for the Atlantic compared to STDR (Fig. 2a and c). Anomalies in the other regions are smaller. The reservoir age shift to higher values in most regions shows that higher diapycnal diffusivity enhances the vertical exchange of deep ^{14}C-depleted waters with the surface ocean. The large drop in reservoir age at the onset of the YD found in both North Atlantic sites has not changed significantly compared to STDR. Thus, the larger MOC drop in DIFF is not reflected in higher reservoir age anomalies.

Finally, the two simulations with additional YD sea ice cover in the Northern Hemisphere are examined. Fig. 2 shows that equivalent ice cover has a substantial effect on reservoir age. As soon as the ice cover appears, the reservoir age rises rapidly in ICE2 (seasonally constant equivalent ice cover north of 56°N), especially in the two North Atlantic regions. The reason for this increase is that during the circulation "off " state, the Arctic waters are not advected away and ^{14}C is prevented from exchanging with the atmosphere. When the circulation recovers, the reservoir age at North Atlantic site E is so high that it is not increased further by the convection induced ventilation of old waters from the deep ocean to the surface. In ICE1, where the equivalent ice cover only appears north of 63°N, the reservoir age rise is less rapid. Interestingly, adding equivalent sea ice cover to CTRL increases reservoir age in the North Atlantic sites only by approximately 50 yr.

These findings are in agreement with the previous modeling work of Schmittner (2003), who finds increased bottom ^{14}C

ages in the global ocean for glacial conditions due to a decrease in air–sea exchange of ^{14}C, which is caused by increased Southern Ocean sea ice cover.

5. Comparison of the model results with reconstructions

Bard et al. (1994), Austin et al. (1995), Haflidason et al. (1995) and Bondevik et al. (2001) have dated the reservoir age at the time of a volcanic ash layer in various sediment cores of the North Atlantic. This ash layer is named the Vedde Ash Bed and has a calendar age of 12.05 to 12.17 ka BP (Bondevik et al., 2006) which places it in the middle of the YD event. In four sediment cores, Bard et al. (1994) measured a reservoir age of 700 to 800 yr (Fig. 6). This is strongly supported by the results of Austin et al. (1995) and Haflidason et al. (1995), who measured a reservoir age of around 700 yr northwest of Scotland and 800 yr southwest of Norway, respectively. Bondevik et al. (2001) obtained a reservoir age of around 600 yr for the west coast of Norway.

Here we compare modeled reservoir age changes for the entire YD period to the reservoir age record of Bondevik et al. (2006) from sediment cores from two basins, which are now bogs, from the Norwegian west coast (at Kulturmyra, 62°20′N 5°39′E and Kvaltjern, 60°25′N 4°59′E) as well as to the results for the Vedde Ash Bed. For the model-data comparison we start with STDR (Fig. 6). It should be noted that the model run starts and ends in a modern state, while the reconstructions have start and end states that are both different from the modern state. Again, we do not take into account the long-term decrease of atmospheric $\Delta^{14}C$ due to possible reductions in ^{14}C production

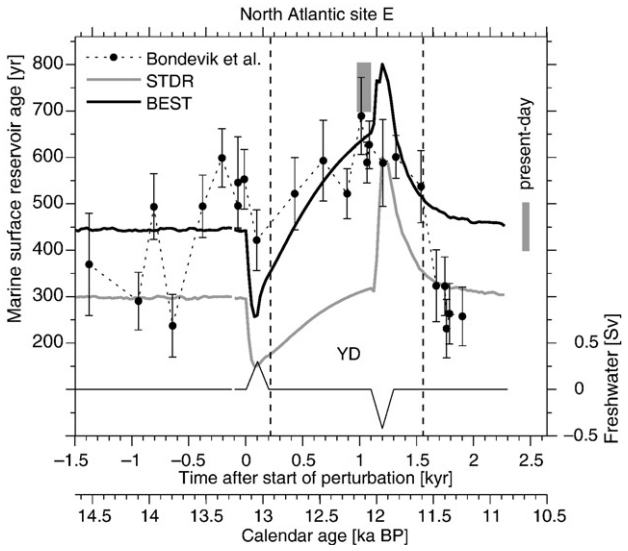

Fig. 6. STDR and BEST reservoir age time series (preceded by a control run) for North Atlantic site E compared to reconstructions by Bondevik et al. (2006) for the YD at the Norwegian west coast (black dots) and by Bard et al. (1994) for the North Atlantic from 40 to 70°N (gray bars, both for present-day and 12 ka BP). In BEST, the reduction of the standard air–sea gas transfer velocity, as used in OCMIP-2 (Orr, 1999), by 19% (Müller et al., in press) and the usage of pre-YD pCO_2 increases reservoir age by approximately 150 yr. The additional sea ice cover during the circulation "off" state results in a faster increase of reservoir age after the initial drop. Model year 0 was pinned to the data such that a good match between model and data was obtained for the YD period.

(Marchal et al., 2001). The modeled results may therefore deviate qualitatively and quantitatively from the reconstructions (as for example at the end of the YD).

From 13.5 to 13.2 ka BP in the Allerød, the reconstructions show reservoir ages of 500 to 600 yr. At the end of the Allerød, the reservoir age decreases by approximately 100 yr. It must be pointed out, though, that only one data point supports this reservoir age decrease. Because the onset of the YD (dotted line in Fig. 6) was dated based on a lithology of various sediment cores (Bondevik et al., 2006), it is not clear whether this reservoir age change is actually due to the MOC slowdown. Model year 0 was pinned to the data by Bondevik et al. (2006) such that a good match between model and data was obtained for the YD period.

STDR starts in a lower, modern state reservoir age and decreases at the onset of the YD due to the MOC shutdown. The rate of reservoir age increase from 12.9 to 12.0 ka BP is well represented by the model. The abrupt MOC recovery in the model simulation leads to a rapid increase in reservoir age to about 600 yr, which is lower than the reconstructed values. The rapidity and magnitude of reconstructed and modeled reservoir age decrease after the MOC recovery are also very similar.

For present-day (pre-bomb) reservoir ages, Bard et al. (1994) find values of 300 to 400 yr for low latitudes and 400 to 500 yr for the North Atlantic from 40 to 70°N. STDR underestimates these values by 100 to 150 yr (Figs. 1a and 6). However, we found that in KGAS, reservoir age is shifted to values about 80 to 100 yr higher (see Section 4) and thus fits much better to the reconstructions for the present-day ocean by Bard et al. (1994). The modeled reservoir age distribution of KGAS also matches fairly well to reservoir age data calculated from the natural $\Delta^{14}C$ of the GLODAP data set (Key et al., 2004). The modeled values are typically 50 to 100 yr lower than the results from GLODAP, though. The match deteriorates in the western Atlantic and in the North Pacific, where the modeled reservoir ages are 200 and 400 yr lower, respectively. For model-data comparison for the YD period, atmospheric pCO_2 of the model should be set as in PCO2. This is not the case in STDR. And although the YD sea ice extent has not been well quantified as yet by paleoclimatic reconstructions, we find it reasonable to add an additional ice cover such as in ICE1. The comparison of the reservoir age reconstructions by Bondevik et al. (2006) with BEST, a simulation which combines KGAS, PCO2 and ICE1 (Table 1, Fig. 6), shows much better agreement than STDR. Note that these results are preliminary because of the highly simplified annual-mean representation of sea ice in the model. Because the reduced air–sea gas transfer velocity in KGAS and reduced pCO_2 in PCO2 merely result in a reservoir age shift, the reservoir age anomalies in Fig. 1 remain valid for KGAS and PCO2.

For the Southern Ocean south of 60°S, Bard et al. (1994) found present-day reservoir ages from 500 to 1200 yr. Simulated reservoir ages in KGAS for this region range from 600 to 1200 yr.

The present-day reservoir ages predicted by our model agree well with the model results by Butzin et al. (2005), who use the Hamburg LSG ocean circulation model. However, for a change in MOC, the surface reservoir age results reported here show considerably better agreement to the observed reservoir age changes in the North Atlantic than the results of Butzin et al. (2005).

6. Conclusions

We find that abrupt changes in ocean circulation, such as a complete shutdown and recovery of the Atlantic MOC, can alter marine surface and bottom reservoir ages by several hundred years. Regions of largest changes (North Atlantic > 50°N and the African west coast) are all affected by modulations of either upwelling strength or vertical mixing. Because the reservoir age changes in these regions are so large, we also find substantial reservoir age variations in the surrounding area of the mentioned locations. Signals of reservoir age anomalies are transported by advection and diffusion. We find a marine surface reservoir age drop of 100 yr at the onset of the YD for the Cariaco Basin and Barbados, which are key paleoceanographic sites where varved sediments and corals are available and used for ^{14}C calibration curves (Hughen et al., 2000, 2006; Fairbanks et al., 2005).

Our model results agree fairly well with present-day and YD reconstructions by Bard et al. (1994) and Bondevik et al. (2006), especially when reducing the air–sea gas transfer velocity by 19%, as suggested by Müller et al. (in press). However, the simulated abrupt marine surface reservoir age increase at the end of the YD is not seen in the reconstructions by Bondevik et al. (2006). There is the possibility that such a transient change of relatively short duration might not be resolved in the records of Bondevik et al. (2006), given the large uncertainties and the limited time resolution of the reservoir age reconstruction. On the other hand, this would support the idea of a rather slow MOC recovery throughout the YD (Stocker et al., 2007) rather than an abrupt recovery at the end of the YD as simulated by this model.

Marine bottom reservoir age anomalies are larger than those of surface reservoir age. The model shows YD bottom reservoir ages up to 1500 yr larger than modern ages in the Caribbean Sea and the Gulf of Mexico, and up to 1700 yr larger south of Greenland. The abrupt MOC recovery leads to a rapid bottom reservoir age drop of 700 to 1000 yr southeast of Greenland.

Parameter sensitivity studies show that increased diapycnal diffusivity tends to result in higher control state (modern) surface reservoir ages, especially in the Pacific with largest anomalies of 200 yr to the North of Australia because of increased vertical mixing. Surface reservoir age changes due to the MOC shutdown are about 50 yr larger in the Atlantic in the simulation with increased diapycnal diffusivity. The differences to STDR are marginal in all other regions.

Increased North Atlantic sea ice cover during the YD has a major effect on reservoir age when the Atlantic MOC is in the "off" mode. In the model a seasonally constant Atlantic equivalent ice cover north of 56°N increases North Atlantic reservoir age by up to 700 yr over 1000 yr, although it is not certain if the sea ice extent during the YD was so far south (Koç et al., 1993). In the model simulation with sea ice cover only north of 63°N, the increase in reservoir age is substantially slower. Due to the very coarse latitudinal resolution of our model at high latitudes and the poorly constrained YD sea ice extent, our simulations with increased sea ice extent only give a first-order estimate of the potential role of sea ice on reservoir age.

In our simulations we were able to show large-scale changes in marine reservoir age in response to abrupt MOC changes and that the effect of sea ice needs to be considered. In this study, the influence of changes in the ^{14}C production rate have not been taken into account. More work needs to be done to better represent sea ice and include ^{14}C production variability in order to estimate their effect on marine surface and bottom reservoir age changes in greater detail.

Acknowledgments

This study was funded by the Swiss National Science Foundation. We thank S. Bondevik for providing his reservoir age reconstructions and comments. We also thank P. Parekh and three anonymous reviewers for many useful comments that helped to improve the paper.

References

Austin, W.E.N., Bard, E., Hunt, J.B., Kroon, D., Peacock, J.D., 1995. The ^{14}C age of the Icelandic Vedde Ash: implications for Younger Dryas marine reservoir age corrections. Radiocarbon 37 (1), 53–62.

Bard, E., Arnold, M., Mangerud, J., Paterne, M., Labeyrle, L., Duprat, J., Méllères, M.A., Sønstegaard, E., Duplessy, J.C., 1994. The North Atlantic atmosphere–sea surface ^{14}C gradient during the Younger Dryas climatic event. Earth Planet. Sci. Lett. 126 (4), 275–287.

Bondevik, S., Mangerud, J., Gulliksen, S., 2001. The marine ^{14}C age of the Vedde Ash Bed along the west coast of Norway. J. Quat. Sci. 16 (1), 3–7.

Bondevik, S., Mangerud, J., Birks, H., Gulliksen, S., Reimer, P.J., 2006. Changes in North Atlantic radiocarbon reservoir ages during the Allerød and Younger Dryas. Science 312, 1514–1517.

Butzin, M., Prange, M., Lohmann, G., 2005. Radiocarbon simulations for the glacial ocean: the effects of wind stress, Southern Ocean sea ice and Heinrich events. Earth Planet. Sci. Lett. 235, 45–61.

Delaygue, G., Stocker, T.F., Joos, F., Plattner, G.-K., 2003. Simulation of atmospheric radiocarbon during abrupt oceanic changes: sensitivities to model parameters. Quat. Sci. Rev. 22, 1649–1660.

Fairbanks, R.G., Mortlock, R.A., Chiu, T.-C., Cao, L., Kaplan, A., Guilderson, T.P., Fairbanks, T.W., Bloom, A.L., Grootes, P.M., M.-J., N., 2005. Radiocarbon calibration curve spanning 0 to 50,000 years BP based on paired $^{230}Th/^{234}U/^{238}U$ and ^{14}C dates on pristine corals. Quat. Sci. Rev. 24, 1781–1791.

Friedrich, M., Remmele, S., Kromer, B., Hofmann, J., Spurk, M., Kaiser, K.F., Orcel, C., Küppers, M., 2004. The 12,460-year Hohenheim oak and pine tree-ring chronology from central Europe — a unique annual record for radiocarbon calibration and paleoenvironment reconstructions. Radiocarbon 46 (3), 1111–1122.

Godwin, H., 1962. Half-life of radiocarbon. Nature 195, 984.

Gulliksen, S., Birks, H.H., Possnert, G., Mangerud, J., 1998. A calendar age estimate of the Younger Dryas–Holocene boundary at Krakenes, western Norway. Holocene 8 (3), 249–259.

Haflidason, H., Sejrup, H.P., Kristensen, D.K., Johnsen, S., 1995. Coupled response of the late-glacial climatic shifts of northwest Europe reflected in Greenland ice cores: evidence from the northern North Sea. Geology 23 (12), 1059–1062.

Hughen, K.A., Southon, J.R., Lehman, S.J., Overpeck, J.T., 2000. Synchronous radiocarbon and climate shifts during the last deglaciation. Science 290, 1951–1954.

Hughen, K.A., Southon, J.R., Bertrand, C.J.H., Franz, B., Zermeño, P., 2004. Cariaco basin calibration update: revisions to calendar and ^{14}C chronologies for core PL07-58PC. Radiocarbon 46 (3), 1161–1187.

Hughen, K., Southon, J., Lehman, S., Bertrand, C., Turnbull, J., 2006. Marine-derived ^{14}C calibration and activity record for the past 50,000 years updated from the Cariaco Basin. Quat. Sci. Rev. 25, 3216–3227.

Karlén, W., Olsson, I.U., Kallberg, P., Kilicci, S., 1964. Absolute determination of the activity of two ^{14}C dating standards. Ark. Geofys. 4, 465–471.

Key, R.M., Kozyr, A., Sabine, C.L., Lee, K., Wanninkhof, R., Bullister, J.L., Feely, R.A., Millero, F.J., Mordy, C., Peng, T.-H., 2004. A global ocean carbon climatology: results from GLODAP. Glob. Biogeochem. Cycles 18.

Koç, N., Jansen, E., Haflidason, H., 1993. Paleoceanographic reconstructions of surface ocean conditions in the Greenland, Iceland and Norwegian seas during the last 14 ka based on diatoms. Quat. Sci. Rev. 12, 115–140.

Kromer, B., Friedrich, M., Hughen, K.A., Kaiser, F., Remmele, S., Schaub, M., Talamo, S., 2004. Late glacial ^{14}C ages from a floating, 1382-ring pine chronology. Radiocarbon 46 (3), 1203–1209.

Levitus, S., Boyer, T., 1994. NOAA Atlas NESDIS 3: World ocean atlas 1994. Tech. Rep. Volume 4: Temperature, U.S. Department of Commerce: National Oceanic and Atmospheric Administration.

Levitus, S., Burgett, R., Boyer, T., 1994. NOAA Atlas NESDIS 3: World ocean atlas 1994. Tech. Rep. Volume 3: Salinity, U.S. Department of Commerce: National Oceanic and Atmospheric Administration.

Marchal, O., Stocker, T.F., Muscheler, R., 2001. Atmospheric radiocarbon during the Younger Dryas: production, ventilation, or both? Earth Planet. Sci. Lett. 185, 383–395.

Meissner, K.J., Schmittner, A., Weaver, A.J., Adkins, J.F., 2003. Ventilation of the North Atlantic Ocean during the Last Glacial Maximum: a comparison between simulated and observed radiocarbon ages. Paleoceanography 18 (2), 1023.

Monnin, E., Indermühle, A., Dällenbach, E., Flücklger, J., Stauffer, B., Stocker, T.F., Raynaud, D., Barnola, J.-M., 2001. Atmospheric CO_2 concentrations over the Last Glacial Termination. Science 291, 112–114.

Müller, S.A., Joos, F., Edwards, N.R., Stocker, T.F., 2006. Water mass distribution and ventilation time scales in a cost-efficient, three-dimensional ocean model. J. Climate 19, 5479–5499.

Müller, S.A., Joos, F., Plattner, G.-K., Edwards, N.R., Stocker, T.F., in press. Modelled natural and excess radiocarbon-sensitivities to the gas exchange formulation and ocean transport strength. Global Biogeochemical Cycles.

Muscheler, R., Kromer, B., Björk, S., Svensson, A., Friedrich, M., Kaiser, K.F., Southon, J., in press. Tree rings and ice cores reveal ^{14}C calibration uncertainties during the Younger Dryas. Nature Geoscience. doi:10.1038/ngeo.XXXX.

Orr, J.C., 1999. On ocean carbon-cycle model comparison. Tellus 51B, 509–510.

Reimer, P.J., Baillie, M.G.L., Bard, E., Bayliss, A., Beck, J.W., Bertrand, C., Blackwell, P.G., Buck, C.E., Burr, G., Cutler, K.B., Damon, P.E., Edwards, R.L., Fairbanks, R.G., Friedrich, M., Guilderson, T.P., Hughen, K.A., Kromer, B., McCormac, F.G., Manning, S., Bronk Ramsey, C., Reimer, R.W., Remmele, S., Southon, J.R., Stuiver, M., Talamo, S., Taylor, F.W., van der Plicht, J., Weyhenmeyer, C.E., 2004. IntCal04 terrestrial radiocarbon age calibration, 0–26 cal kyr BP. Radiocarbon 46, 1029–1058.

Schmittner, A., 2003. Southern Ocean sea ice and radiocarbon ages of glacial bottom waters. Earth Planet. Sci. Lett. 213, 53–62.

Southon, J., 2004. A radiocarbon perspective on Greenland ice-core chronologies: can we use ice cores for C-14 calibration? Radiocarbon 46 (3), 1239–1259.

Stocker, T.F., Wright, D.G., 1996. Rapid changes in ocean circulation and atmospheric radiocarbon. Paleoceanography 11, 773–796.

Stocker, T.F., Wright, D.G., 1998. The effect of a succession of ocean ventilation changes on ^{14}C. Radiocarbon 40 (1), 359–366.

Stocker, T.F., Timmermann, A., Renold, M., Timm, O., 2007. Effects of salt compensation on the climate model response in simulations of large changes of the Atlantic meridional overturning circulation. J. Climate 20, 5912–5928.

Stuiver, M., Braziunas, T.F., 1993. Modeling atmospheric ^{14}C influences and ^{14}C ages of marine samples to 10,000 BC. Radiocarbon 35 (1), 137–189.

Tarasov, L., Peltier, W.R., 2005. Arctic freshwater forcing of the Younger Dryas cold reversal. Nature 435 (2), 662–665.

Walsh, J., 1978. A data set on Northern Hemisphere sea ice extent, 1953–1976. Glaciological Data, World Data Center for Glaciology (Snow and Ice), Report GD-2, pp. 49–51.

Zwally, H.J., Comiso, J., Parkinson, W., Campbell, W., Carsey, F., Gloerson, P., 1983. Antarctic Sea Ice, 1973–1976: Satellite Passive Microwave Observations. NASA. 206 pp.